JOURNAL OF NEUROPHYSIOLOGY
Vol. 61, No. 5, May 1989. *Printed in U.S.A.*

Role of Extracellular Space in Hyperosmotic Suppression of Potassium-Induced Electrographic Seizures

STEPHEN F. TRAYNELIS AND RAYMOND DINGLEDINE
Department of Pharmacology, University of North Carolina, Chapel Hill, North Carolina 27514

SUMMARY AND CONCLUSIONS

1. Focal electrographic seizures arose in the CA1 region of rat hippocampal slices bathed in elevated (8.5 mM) external potassium ($[K^+]_o$). High $[K^+]_o$ also induced spontaneous interictal bursts that originated in area CA3 and propagated to CA1. To examine the contribution to electrographic seizure initiation of excitatory mechanisms that are influenced by extracellular volume, we studied the effect of hyperosmotic expansion of interstitial volume on seizure occurrence, interictal bursts, and excitatory synaptic transmission. The tissue electrical resistance was also measured leading up to and during seizures.

2. Media made 5–30 mosmol/kg hyperosmotic by addition of agents restricted to the extracellular space (mannitol, sucrose, raffinose, L-glucose, dextran) rapidly and reversibly abolished $[K^+]_o$-induced spontaneous CA1 seizures in 86% of slices tested. However, similar increases in osmolality effected by agents that access the intracellular compartment (D-glucose, glycerol) did not influence electrographic seizure occurrence. Hyperosmotic changes with plasma membrane impermeable compounds, but not permeable compounds, produced significant concentration-dependent decreases (1–10%) in the electrical resistance of CA1 stratum pyramidale. Because tissue resistance is proportional to extracellular volume, these results suggest that hyperosmotic suppression of electrographic seizures is associated with expansion of the extracellular space in hippocampal slices.

3. Measurement of electrical resistance of the CA1 stratum pyramidale during spreading depression and electrographic seizure revealed an increase in tissue resistance to 122% and 108% of control, respectively. Furthermore, a slight (~2%) but significant increase in electrical resistance gradually occurred over the 20 s immediately preceding seizure generation. The observed increase in tissue resistance suggests extracellular space is decreased during these events.

4. Hyperosmolality did not alter CA3 interictal burst frequency. However, burst intensity, estimated from the total length of the burst waveform, was significantly reduced in both the CA3 (83% control) and CA1 region (67% control) when osmotic changes were imposed by plasma membrane impermeant compounds. Additionally, media made hypoosmotic by removal of 7.5 mM NaCl reversibly increased burst intensity.

5. High $[K^+]_o$ potentiated excitatory synaptic transmission and excitatory postsynaptic potential (EPSP) spike coupling. Increases in osmolality sufficient to block electrographic seizures did not dramatically alter excitatory synaptic transmission between the Schaffer/commissural system and CA1 neurons, as judged by input-output curves relating the field EPSP to presynaptic fiber volley. Likewise, hyperosmotic manipulations in either 3.5 or 8.5 mM $[K^+]_o$ did not change the shape or position of the input-output curve relating CA1 population spike to field EPSP; however, hyperosmolality significantly reduced the maximum population spike amplitude.

6. These results suggest that extracellular space plays a key role in regulating the excitability of CA1 neurons bathed in high $[K^+]_o$. The apparent reduction in extracellular space that occurs before and during seizures probably increases neuronal synchrony and excitability by enhancing the spatial effectiveness of electric fields (ephaptic coupling) and exaggerating transient elevations in extracellular $[K^+]_o$ produced by neuronal activity. We suggest these effects act in concert to promote the conditions necessary for seizure initiation within CA1.

INTRODUCTION

Two forms of spontaneously occurring epileptiform activity are generated in hippocampal slices perfused with media containing elevated (8 5 mM) $[K^+]_o$. Electrographic seizures, 20–90 s in duration with both tonic- and clonic-like components, appear in and are restricted to the CA1 field (66). In addition, interictal bursts, 50–100 ms in duration, arise predominantly in the CA3b or CA3c subfield and propagate synaptically to CA1 pyramidal cells (33, 52). In slices bathed in 1.5 mM $[Ca^{2+}]_o$ and $[Mg^{2+}]_o$, the CA3 interictal input triggers CA1 seizure initiation; however, slight reductions in external divalent cations render seizure occurrence independent from interictal input (65). Electrographic seizures in high $[K^+]_o$ begin with a tonic component that appears similar to the ictallike events observed in hippocampal slices perfused with media containing very low $[Ca^{2+}]_o$ (28, 31, 62). This is followed by a synaptically driven clonic phase containing large-amplitude bursts followed by afterdischarges (66). An understanding of the cellular mechanisms responsible for electrographic seizure initiation in slices bathed in high $[K^+]_o$ would help clarify the relevance of this in vitro model to seizures in intact animals and may provide some insight into mechanisms of seizure initiation in situ. In this paper we demonstrate that reductions in extracellular space contribute to excitatory processes that allow the interictal trigger arriving from CA3 to excite and synchronize a sufficient number of CA1 neurons into seizure.

$[K^+]_o$ rises during experimental seizures in situ and in vitro and has long been debated as a contributive factor to seizure initiation and maintenance (9, 14, 15, 24, 55, 74). High $[K^+]_o$ can increase tissue excitability in multiple ways. In addition to neuronal depolarization and reduction in K^+ driving force, elevated $[K^+]_o$ reduces chloride-mediated GABAergic inhibitory postsynaptic potentials (IPSPs) (33, 40) and K^+-mediated afterhyperpolarizations (1); *N*-

methyl-D-aspartate (NMDA) receptor activation should be enhanced by the cumulative depolarization (44). High $[K^+]_o$ also produces temperature-dependent glial swelling in situ (e.g., Ref. 4), and the consequent reduction in extracellular space should increase tissue excitability (12, 13). However, activation of the Na/K ATPase (54) and a tendency towards axonal conduction block in high $[K^+]_o$ (50) may partially offset the rise in neuronal excitability. Elevated $[K^+]_o$ also seems to be a common denominator among several in vitro preparations that exhibit seizurelike activity. Electrographic seizures observed in hippocampal or neocortical slices (from neonatal rats) bathed in $GABA_A$ antagonists occur with $[K^+]_o$ elevated to 5.0 mM (22, 60). $[K^+]_o$ also rises during washout of $[Ca^{2+}]_o$ in hippocampal slices (73) and application of 4-aminopyridine (4-AP) to olfactory cortical slices (17). Elevations in $[K^+]_o$ increased the occurrence of stimulus-induced seizures in hippocampal slices (56), and similar stimulus-induced seizures in situ are preceded by a rise in extracellular $[K^+]_o$ to ~8.0 mM during stimulation (57). Finally, some of the excitatory actions of kainate on nervous tissue might be a consequence of increased $[K^+]_o$, because kainate can induce an efflux of K^+ from glia (37). Perhaps not surprisingly, the characteristics of seizures are often similar in these different preparations, which suggests the fundamental events that lead to seizure initiation and termination might also be similar.

We have hypothesized that K^+-induced glial swelling and the consequent reduction in extracellular space might contribute significantly to the cycle of events that leads to seizure initiation in the high $[K^+]_o$ model (66). Reduction in extracellular space caused by elevated $[K^+]_o$, such as that observed in optic nerve and cerebral cortex (11, 51), could increase neuronal excitability by exaggerating transient changes in extracellular ion activities or enhancing electric field interactions (12, 13). To examine the potential contribution of potassium-induced reduction in extracellular space to high $[K^+]_o$-induced epileptiform activity, we tested the effect of osmotic manipulations on electrographic seizures and interictal bursts and also measured tissue resistance over the seizure time course. Our results suggest that small changes in osmolality imposed by agents that do not readily cross cell membranes suppress CA1 electrographic seizures quickly and reversibly, and that tissue resistance rises prior to and during electrographic seizures. Some of these results have been reported in preliminary form (67, 68).

METHODS

Hippocampal slices (450 μm thick) were prepared from the central four-fifths of the hippocampus as previously described (66). Rat age ranged between adolescence (1.5 mo) to adult (4 mo), and was not correlated with seizure propensity ($r = 0.1$; $n = 48$ rats). In some experiments, CA1 minislices were obtained by removing the CA3 region with a razor blade chip immediately after slicing. Slices were held in an interface recording chamber and perfused via a syringe pump at a rate of 0.5 ml/min with the following medium (in mM): 130 NaCl, 24 $NaHCO_3$, 3.5 KCl, 1.25 NaH_2PO_4, 1.5 $CaCl_2 \cdot 2H_2O$, 1.5 $MgSO_4 \cdot 7H_2O$, and 10 glucose, equilibrated with 95% O_2–5% CO_2 to a pH of 7.4. $[K^+]_o$ was elevated from 3.5 to 8.5 or 9.0 mM by adding 0.0050 or 0.0055 volumes of 1 M KCl to the normal medium. Calcium activity, as measured by a calcium-sensitive electrode (Radiometer-Copenhagen), was 1.4 ± 0.03 mM ($n = 22$). In some experiments $[Ca^{2+}]_o$ and $[Mg^{2+}]_o$ were reduced by partial removal of $CaCl_2$ and $MgSO_4$. Warmed, humidified 95% O_2–5% CO_2 flowed over the surface of the slices at a rate of 400 ml/min, and the bathing medium was maintained at a temperature of 35.0–37.5°C unless stated otherwise. Extracellular recordings were made with micropipettes (15–30 MΩ) filled with 0.9% NaCl. Potentials were led through a DC electrometer, displayed on an oscilloscope and chart recorder, and stored on FM tape and flexible disks of a DEC PDP 11/23 or IBM compatible 80386-based computer. Our typical recording sites are shown in Figs. 1A, 2A.

Osmotic manipulations

The neutral polyhydroxy alcohols and sugars used to raise osmolality are of two classes: compounds nearly restricted to the extracellular space that change transmembrane osmotic pressures, and compounds that freely access the intracellular compartment and, therefore, exert no net osmotic effect. L-glucose, mannitol, sucrose, and dextran (~10,000 D; i.e., ~60 D-glucose residues) are restricted to the extracellular compartment in the CNS (23, 45, 53), and the trisaccharide raffinose should behave similarly. Hyperosmotic shrinkage of cell volume with these compounds has been documented in endothelial cells (e.g., Ref. 58), peripheral nerves (59), and cortical slices (46), and also inferred in situ from measurements of intracranial pressure and brain water content (e.g., Ref. 49). In contrast, glycerol equilibrates across the plasma membrane in peripheral tissue by means of both rapid ($t_{1/2}$ of ~5 s in red blood cells), carrier-facilitated and slow, nonspecific diffusion paths (5, 36), and reaches brain intracellular compartments within minutes of intraventricular injection (45). D-glucose rapidly crosses the plasma membrane of blood vessel endothelial cells and, apparently, neurons and glia (10) via the stereoselective, cytochalasin-sensitive, Na^+- and energy-insensitive glucose transporter (20, 23). All compounds were chosen for their osmotic properties, but some possess other actions such as alterations in membrane transport systems, cellular metabolism, and protein synthesis (6, 47, 61, 63).

Hyperosmotic solutions were made by direct addition of the appropriate amount of compound to the media; hypoosmotic changes were produced by omission of 7.5 mM NaCl. Osmolality was measured in triplicate on a *Micro Osmometer* (Precision Systems), and was 312 ± 0.6 ($n = 34$) and 321 ± 0.7 ($n = 35$) mosmol/kg for media with 3.5 and 8.5 mM $[K^+]_o$, respectively. The average difference between calculated and measured osmotic changes was 12.6%; the mean and calculated values for each series were not significantly different; therefore, changes in osmolality reported in RESULTS indicate calculated changes. Hyperosmotic manipulations did not influence solution conductance. Our perfusion system had a dead time of 2.0 min, after which new solutions entered a 2.5-ml compartment before reaching the slices. Solution at the slice should be >97% replaced within 15 min of switching perfusate, if mixing is rapid. The effect of hyperosmolality on spontaneous epileptiform activity was assessed by recording for 20–30 min during a control period, 20–30 min during perfusion of hyper- or hypoosmotic media, followed by 20–40 min over recovery.

Analysis of interictal bursts

The relative intensity of spontaneous interictal bursts was quantified with a procedure first described by Korn et al. (33). Spontaneous bursts were captured by an event-triggered analog delay circuit and digitized at 5–10 kHz. The total length of the line comprising the burst waveform was calculated, and an ap-

propriate length measured from a burst-free segment of the recording was subtracted. The resulting digital value, termed the "coastline burst index," is correlated with the subjective intensity of the burst. Under most conditions this index would be expected to increase if neuronal synchrony, burst duration, number of participating neurons, or firing frequency increased. Although this measure does not distinguish among these potential mechanisms, it does provide a sensitive indicator of burst intensity that lends itself well to statistical analysis. Burst waveforms were also examined by counting the number of constituent population spikes (25–80 bursts per experimental period); population spikes could be resolved from background noise to within ±1 per burst.

Measurement of tissue resistance

The electrical resistance of the tissue was evaluated using a modification of the method described by Holsheimer (26). An electric field was produced simply by passing a biphasic square current pulse (5–15 ms duration; ±1–2 μA; 1.0 Hz) between two sharpened tungsten electrodes positioned 1.1–1.5 mm apart in the CA1 stratum pyramidale at a depth of 150–250 μm (Fig. 1*A*). Two glass micropipettes positioned 150–250 μm apart between the stimulating electrodes at a depth of 150–250 μm differentially recorded the voltage drop during stimulation (Fig. 1*B*). The intensity of the current pulses was well below that able to evoke population spikes; the recorded electric field was below 4 mV/mm, or less than that found to alter population spikes in granule cells (27). Recordings were typically filtered at 100–400 Hz; in some experiments current pulses were shaped through a 4.7-nF capacitor to minimize stimulus artifacts. Holsheimer (26) found that the voltage drop with sinusoidal currents was the same at 100 and 1,000 Hz stimulation and concluded that the volume conductor was primarily resistive rather than capacitive. To further verify that the amplitude of voltage deflections we observed with this modified technique reflected resistance between the glass micropipettes (i.e., the system obeyed Ohm's Law), we manipulated ionic strength or stimulus current and recorded the magnitude of the differential voltage. The steady voltage drop between the recording electrodes was linearly dependent on stimulus current in both tissue (Fig. 1*C*) and saline ($r = 0.934$; $n = 11$ observations; $P < 0.001$). Similarly, Fig. 1*D* illustrates the near linear relationship between the reciprocal of the relative voltage drop in saline and the solution conductance measured using a conductance bridge (Yellow Springs Instrument Co.). A linear relationship ($r = 0.994$; $n = 12$ observations; $P < 0.001$) was also found between the voltage drop and the distance between the recording micropipettes, which indicates that the recording distance (50–325 μm) was large enough to smooth out any microscopic fluctuations in tissue resistance. Thus, in three experimental situations the voltage deflection behaved as predicted by Ohm's Law, suggesting this technique does provide a measure of tissue resistance, although it apparently underestimates moderate decreases in conductance (Fig. 1*D*). It was not possible to derive absolute values of tissue resistance because of uncertainties in electric field geometry for a spatially restricted environment, and in current density between our point current sources. Therefore, no attempt was made to describe the absolute resistance of tissue under any one set of circumstances; instead, the magnitude of the voltage deflection was always described as a relative value.

The amplitudes of the voltage deflection during each component of the biphasic pulse were measured for 20–40 min in slices not undergoing electrographic seizures (temperature, 32–35°C) to ensure that a stable base line existed, and subsequently averaged for 75–250 stimulus pulses during control, hyperosmotic, and recovery periods. Measurements that fell coincident with interictal bursts or population spikes during seizures were disregarded, because the accompanying rapid changes in field potential and $[K^+]_o$ complicated interpretation. Following some experiments, the electrode assembly was moved from slice to bath and the resistance measured. The voltage deflection in the bath was 24.4 ± 4.7% ($n = 10$) of that in tissue, as expected if most of the current flow within the tissue occurred in the extracellular fluid. To evaluate tissue resistance over the interseizure interval and during electrographic seizures, current pulses were applied at 1 Hz in 12 slices undergoing spontaneous seizures (24 ± 3.8 seizures per slice), and measurements of differential voltage drops aver-

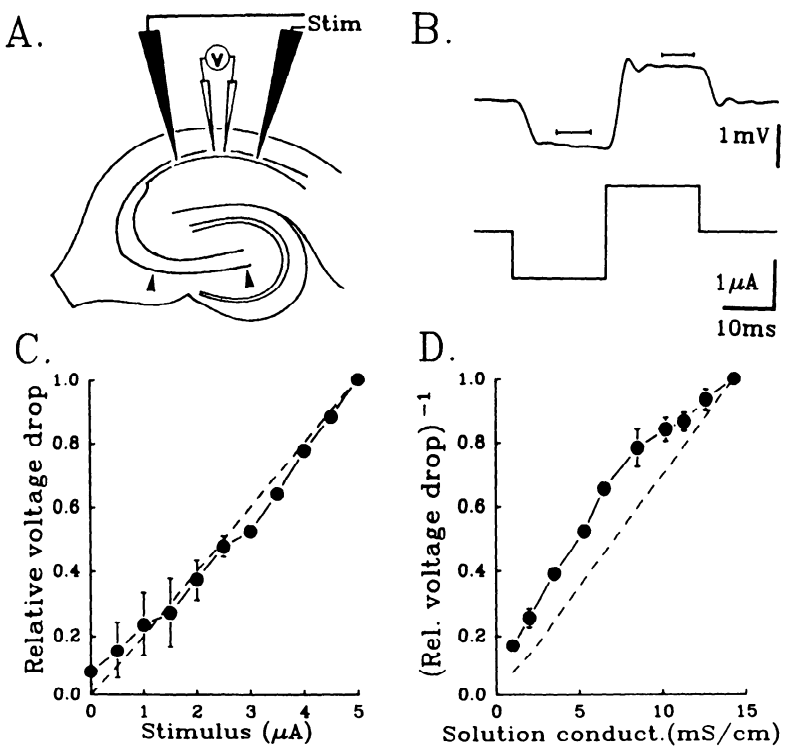

FIG. 1. Analysis of electrical tissue resistance. *A*: this diagram illustrates the arrangement of electrodes used to measure electrical resistance within CA1 stratum pyramidale. Outer electrode pair (solid) represent sharpened tungsten stimulating electrodes, and inner pair (open) indicate recording micropipettes placed in area CA1b; arrows denote CA3b/c burst generator. *B, top*: typical differential voltage drop (average of 30 sweeps; low-pass filtered at 200 Hz) recorded between the micropipettes during a biphasic current pulse (1.0 Hz; *lower*) applied across the metal electrodes. Bracketed portions of the voltage trace indicate where the amplitude of deflection was measured for reference to prestimulus value. *C*: a plot of stimulus intensity vs. relative voltage drop in tissue was linear ($r = 0.993$; $P < 0.001$). *D*: likewise, the relationship between solution conductance (measured with a conductance bridge) and the reciprocal of the differential voltage deflection recorded in bath was linear ($r = 0.984$; $P < 0.001$). Each point in *C* and *D* represents the average of values from 6 experiments. Broken lines: predicted linear relationship in each case; error bars show SE when larger than symbol size. Experiments in *C* and *D* together verify that the voltage deflections recorded obey Ohm's Law and are, therefore, proportional to tissue resistance.

aged together in the following manner. The result of sampling resistance continually in a single slice was an array of measured values; segments of this array that included a single seizure plus ~1 min before and after were identified. These segments were aligned on the moment of seizure initiation, which was defined (within ±1 s) as the sharpest drop in the DC field potential (66) and averaged point for point. The resulting time courses of resistance for each slice were subsequently averaged together to produce a composite record of resistance over seizure time course that represented all slices equally.

Evaluation of excitatory CA1 synaptic transmission

Excitatory synaptic transmission between the Schaffer/commissural system and CA1 pyramidal cells was examined under hyperosmotic conditions in both 3.5 and 8.5 mM $[K^+]_o$. For these experiments, the temperature was held at 32.0–34.0°C to discourage seizure occurrence (66). Orthodromic stimulation (100-μs square pulses; 1–150 μA) was applied every 2–5 s through a sharpened tungsten monopolar electrode positioned amidst afferent fibers in stratum radiatum. An extracellular micropipette placed in the stratum radiatum recorded the presynaptic fiber volley and field EPSP; a second micropipette in the CA1 stratum pyramidale recorded the population spike. Figure 2*A* shows our typical recording sites. Figure 2*B* illustrates the waveform of the field potentials recorded from the dendritic and cell body layers and demonstrates how each parameter was measured. The peak-to-peak amplitude of the fiber volley and population spike were accurate indicators of the magnitude of these events, but the peak of the field EPSP is contaminated by the population spike dipole. Consequently, we used the slope of the initial portion of the EPSP as an indicator of its magnitude, because this measure is only influenced by an invading population spike at higher stimulus intensities. Input-output curves of the population spike amplitude as a function of the EPSP slope (EPSP-spike curve) and EPSP slope as a function of presynaptic fiber volley amplitude (volley-EPSP curve) were generated by increasing the stimulus intensity manually in small increments and measuring on-line the desired parameters from waveforms digitized at 5–10 kHz. Data for two input-output curves (typically 100–125 data points each) were collected 10–15 min apart, and only slices with minimal variability between these control curves were studied further. Subsequently, input-output curves were generated following application of hyperosmotic medium for 20–25 min and, likewise, after a 20- to 25-min recovery period.

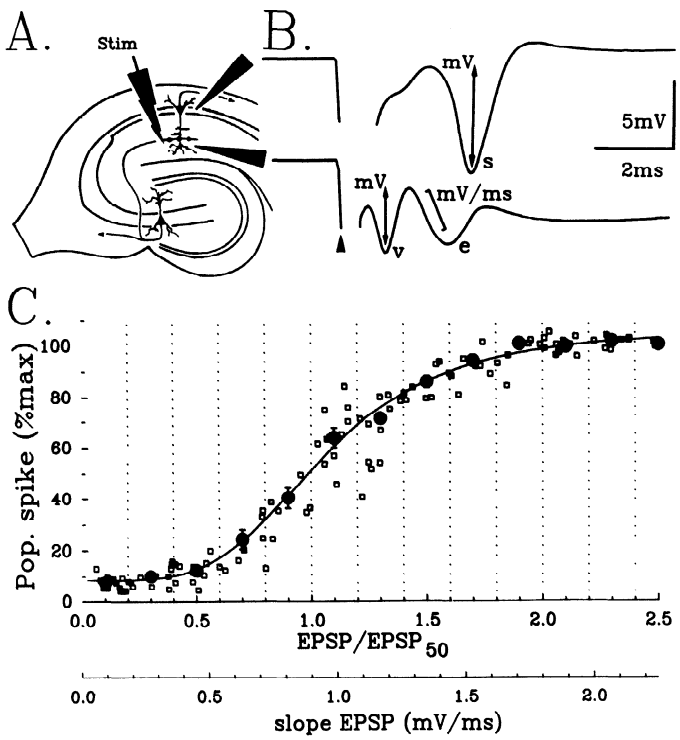

FIG. 2. Evaluation of synaptic transmission and EPSP-spike coupling in CA1. Diagram in *A* illustrates our recording sites and the Schaffer collateral projection from CA3 to CA1 (not drawn to scale). *B*: typical waveform of an orthodromically stimulated population spike recorded from stratum pyramidale (labelled "s"; *top*) and a dendritic recording of fiber volley ("v"; *lower*) and field EPSP ("e") are shown (average of 30 sweeps; arrowhead marks onset of stimulus artifact). Vertical arrows indicate how peak-to-peak values (mV) were measured for the population spike and presynaptic volley amplitudes. Initial portion of the field EPSP (bracketed) was fit to a line and the slope calculated (mV/ms). *C*: this scatter plot (open squares) represents raw data describing EPSP-spike relationship from a single slice before binning (see METHODS). *Top axis* on *abscissa* is the EPSP slope expressed as a ratio to that which elicits a half-maximal population spike ($EPSP_{50}$; Ref. 69); lower scale contains the raw EPSP slope values. Vertical dashed lines mark different bins (chosen at 0.2 $EPSP/EPSP_{50}$), and average (large closed circles) of all data points within each bin was placed at the bin center. Error bars indicate SE when larger than symbol size. Curves fit to the raw or averaged data (METHODS) were identical.

The effect of hyperosmotic manipulations on synaptic transmission was estimated by calculating the slope of the volley-EPSP curve that was generated in hyperosmotic media. For each slice, the slope of this curve was expressed as a percent of the average slope in the control and recovery periods and the resulting values from a number of slices averaged together. To examine the effect of hyperosmotic media on the EPSP-spike curves in a population of slices, data from different slices were normalized and averaged as follows. The population spike was expressed as a fraction of its maximal value, and the field EPSP as a ratio to that which elicited a half-maximal population spike (the so-called $EPSP_{50}$; Ref. 69). Because population spikes were evoked at irregular EPSP values, the data points from each slice were binned to express the population spike amplitude at regular EPSP intervals. This was accomplished by replacing all data points within every 20% of the normalized EPSP with their average placed at the bin center (see Fig. 2*C*). Subsequently, these records were averaged among slices to produce a composite plot representative of all slices (e.g., Fig. 5).

Statistical evaluation

To compensate for slow changes in measured parameters over time, all measured values during osmotic manipulations were expressed as a percent of the average of the control and recovery measurements (±SE). The mean values for measurements of parameters among a population of slices were evaluated for significance using a paired or unpaired Student's *t* test, as appropriate. Differences were considered significant at the 95% confidence level ($P_{\alpha/2} < 0.05$). When values were not significantly different, the power ($1 - \beta$) of the statistical test was calculated and was typically >0.8 for detection of a real 5% difference. Correlative data were fit by linear regression (least squares), and inferences about the fit estimated from the correlation coefficient. Data points comprising composite EPSP-spike curves were fit to the equation

$$\text{Population spike} = \{[\max - \min]/[1 + (\text{EPSP}/\text{EPSP}_{50})]^s\} - \min$$

where max and min represent the maximum and minimum population spike amplitude, respectively. This equation was solved for max, min, $EPSP_{50}$, and the slope factor s by nonlinear regression using a simplex algorithm (least squares), given input values for the normalized EPSP and population spike amplitude. $EPSP_{50}$

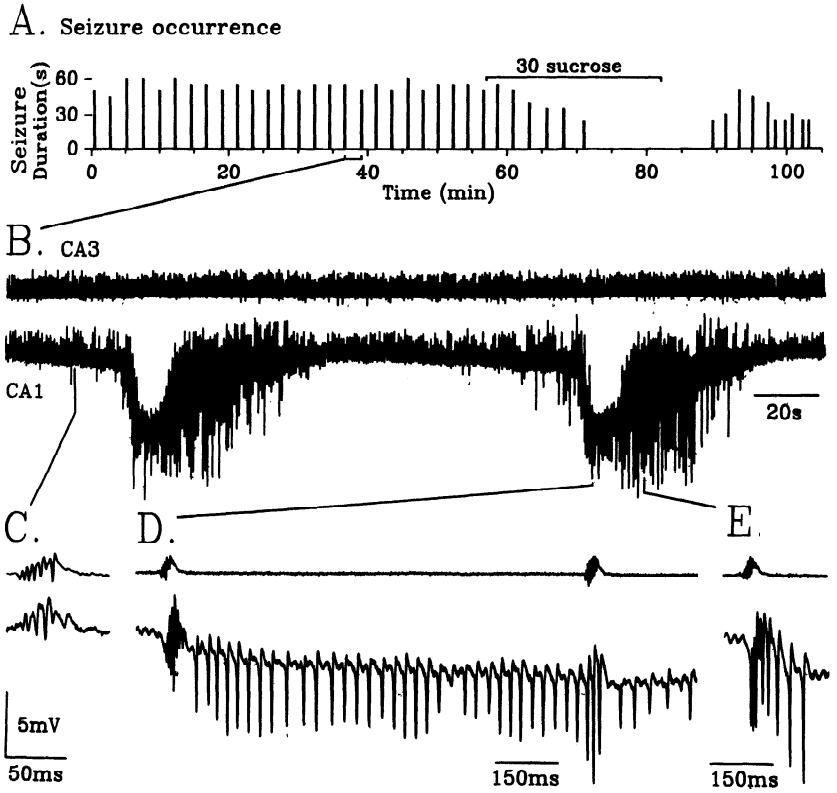

FIG. 3. Hyperosmotic suppression of high $[K^+]_o$-induced electrographic seizures. *A*: this time line illustrates the occurrence of seizures over a period of ~2 h in a single slice. Position of each vertical bar represents the moment of seizure occurrence, and amplitude denotes seizure duration. Sucrose (30 mosmol/kg) was added to the media during the time indicated. *B*: time scale expansion of a simultaneous recording from the CA3 (*top*) and CA1 (*bottom*) regions during two seizure episodes, as indicated on the time line. Note seizures appear nearly identical, and each is composed of 2 distinct phases. *C*: expansion of a single, interictal burst prior to seizure initiation, as shown in *B*. *D*: expansion of the initiation and tonic phase as illustrated in *B*. *E*: expansion of a single burst during the clonic phase, as indicated in *B*. Note bursts during the clonic phase *E* were followed by 100 to 200-ms afterdischarges, and burst intensity in CA1 was considerably greater than during the interictal period *C*. Traces in *D* and *E* are on the same time scale; traces in *C* are expanded.

was used to gauge the lateral position of the input-output curves, and max used to estimate maximum population spike amplitude.

RESULTS

Hippocampal slices bathed in 8.5 mM $[K^+]_o$ generated two different forms of spontaneous epileptiform activity, as previously described (66). Short-duration (50- to 100-ms) interictal bursts arose in the CA3 region and propagated throughout the pyramidal cell subfields in 71% of 782 slices tested (e.g., Fig. 3*C*). Additionally, in 17% of 554 slices that generated spontaneous bursts, electrographic seizures (subsequently referred to as "seizures") recurred spontaneously and exclusively in the CA1 region (Fig. 3, *A* and *B*). Seizures were comprised of two distinct phases: a toniclike phase (duration, 1–10 s) that consisted of prolonged and synchronous firing (Fig. 3*D*) and a cloniclike phase (duration, tens of seconds) composed of exaggerated interictal bursts followed by 100–200 ms afterdischarges (Fig. 3*E*). Average interseizure interval and seizure duration were 2.5 ± 0.1 min (n = 94) and 49.0 ± 4.0 s (n = 95), respectively. These mean values did not differ significantly from those previously reported for a different population of 192 slices undergoing electrographic seizures (66).

Hyperosmotic suppression of electrographic seizures

To determine whether excitatory processes dependent on the volume of extracellular space contribute to high $[K^+]_o$-induced seizure generation, we manipulated interstitial volume osmotically via inclusion of various membrane impermeable compounds in the bathing media. High $[K^+]_o$-induced electrographic seizures were rapidly abolished in 48 of 56 slices in media made 5, 15, or 30 mosmol/kg hyperosmotic by addition of agents restricted to the extracellular space (Table 1; Fig. 3*A*). These manipulations represent increases in osmolality of 2.0–10.3%. Prior to seizure suppression, hyperosmotic solutions often lengthened interseizure interval and attenuated seizure duration (e.g., Fig. 3*A*). Seizure suppression usually occurred within the time our perfusion system required to replace 97% of the media (15 min), and seizure activity was rein-

TABLE 1. *Effects of hyperosmolality on electrographic seizures*

	Increase in Osmolality, mosmol/kg*	CA1 Seizures Stopped
Impermeant Compounds†		
Mannitol	+5, 15, 30	21/23‡
Sucrose§	+5, 15, 30	13/15‡
Raffinose	+15	4/7‡
L-Glucose	+15	4/5‡
Dextran	+15	6/6‡
Pooled		48/56‡
Permeant Compounds†		
Glycerol	+30	1/13
D-Glucose	+30	3/12
Pooled		4/25

*Medium was made hyperosmotic by direct addition of appropriate amount of compound (see METHODS). For both mannitol (m) and sucrose (s), three concentrations were utilized: 5 (n_m = 7; n_s = 4), 15 (n_m = 6; n_s = 3), and 30 (n_m = 10; n_s = 8) mosmol/kg. †Impermeant and permeant refer to compound's ability to access intracellular compartment via passive transport. ‡$P < 0.05$; significantly different from proportion of slices undergoing electrographic seizure during both control and recovery period, test of proportions. Power for detecting a change of 0.25 was >0.73. §Three slices, in which 30 mM sucrose reversibly abolished seizures, had been previously treated with 10 μM D-2-amino-5-phosphonovaleric acid with no effect on seizures.

TABLE 2. *Hyperosmotic effects on electrical resistance in CA1 stratum pyramidale*

	Percent Change	
	Tissue resistance*	Medium osmolality†
Mannitol, 5 mM	−1.2 ± 0.47‡ (11)	+2.0 ± 0.42‡ (8)
Mannitol, 15 mM	−5.3 ± 1.27‡ (7)	+4.7 ± 0.26‡ (11)
Mannitol, 30 mM	−8.9 ± 0.81‡ (6)	+10.1 ± 0.35‡ (16)
Glycerol,§ 30 mM	+2.0 ± 0.89 (7)	+10.3 ± 0.20‡ (6)

Numbers in parentheses indicate number of slices or media tested. *Measurements were made over 75–250 stimulus pulses in each period. Data were converted to mean of control and recovery measurements, averaged together, and expressed as difference from 100% (±SE). †Measured osmolality was expressed as percent of control, which overall was 321 ± 0.7 mosmol/kg (n = 35) for media containing 8.5 mM $[K^+]_o$. Measurements were drawn from experiments in addition to those in which resistance was measured. ‡$P < 0.05$; significantly different from 0% change by Student's t test. §For glycerol, the power to detect a real 2% change in tissue resistance was 0.75.

stated in 39 of 48 slices by return to normoosmotic conditions (e.g., Fig. 3*A*). Increases in osmolality of 5, 15, or 30 mosmol/kg were all equally effective at suppressing seizure. However, seizures were abolished more quickly at higher (30 mosmol/kg) concentrations of sucrose or mannitol.

We investigated the effect of hyperosmolality in several additional situations in which 8.5 mM $[K^+]_o$ induced electrographic seizures. Electrical stimulation of CA1 afferents in CA1 minislices with the CA3 burst generator surgically removed produces spontaneous seizures similar to those in whole slices (66). Media made hyperosmotic by addition of 15–30 mosmol/kg mannitol abolished seizures in 8 of 11 such stimulated minislices, and this effect was reversible in 5 of 8 slices. In addition, slight reduction of external divalent cations from 1.5 to 1.2 mM renders seizure initiation independent of interictal input (65), and under these conditions, hyperosmolality (15 mosmol/kg mannitol) reversibly abolished seizures in 6 of 13 slices. Similarly, spontaneous discharges that occur in isolated CA1 minislices bathed in 1.2 mM $[Ca^{2+}]_o$ and $[Mg^{2+}]_o$ (65) were reversibly abolished in 3 of 12 slices by 15 mosmol/kg mannitol.

Hyperosmotic conditions were also imposed with D-glucose and glycerol, which access the intracellular compartment via facilitated diffusion. When tested at 30 mosmol/kg, neither D-glucose nor glycerol influenced seizure occurrence (Table 1). Glycerol had no effect on seizure appearance, although D-glucose transiently attenuated seizure duration and lengthened interseizure interval in some slices. This might reflect transient changes in osmotic pressure associated with the initial presentation of 30 mM D-glucose to the cells, because D-glucose probably traverses cell membranes somewhat more slowly than glycerol (20, 36).

Hyperosmotic reduction in tissue resistance

To investigate whether hyperosmotic manipulations actually changed extracellular volume in hippocampal slices as in other tissues, we measured osmolality-induced changes in tissue resistance, because this parameter should be inversely related to the volume of extracellular space (Ref. 18; see DISCUSSION). The addition of mannitol to slices bathed in 8.5 mM $[K^+]_o$ reversibly decreased tissue resistance in a dose-dependent manner (Table 2). In contrast to 30 mosmol/kg mannitol, glycerol (30 mosmol/kg) did not significantly affect tissue resistance. These experiments imply that media made hyperosmotic by addition of compounds that alter transmembrane osmotic pressure expand extracellular volume, whereas hyperosmotic manipulations with compounds that access the intracellular compartment do not. An important prediction from these results is that the amplitude of extracellular field potential recordings should be attenuated by osmotic changes in tissue resistance. Such reductions should be independent of

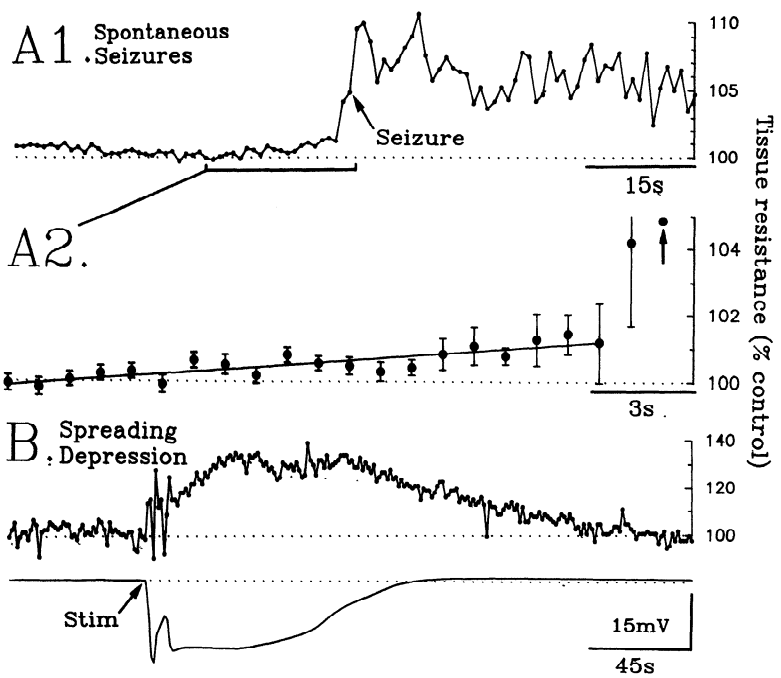

FIG. 4. Tissue resistance during electrographic seizures and spreading depression. *A1*: tissue resistance was sampled at 1 Hz in 12 slices over a total of 286 seizures, and the resulting arrays of measured values were averaged as described in METHODS. *Ordinate*: percent of the value 20 s before seizure onset; arrow: time of seizure occurrence, determined within ±1 s. *A2*: expansion of 20-s period immediately preceding seizure onset illustrates the gradual and significant increase in resistance, suggesting extracellular space might decrease prior to seizure initiation. Line: linear regression over these 20 values; error bars: SE for 12 values. For comparison, traces in *B* illustrate tissue resistance and field potential measured over time course of spreading depression produced by <1 s orthodromic stimulation (100 Hz; 100 μA; see arrow) in a single slice. Again, resistance is referenced to its value 20 s prior to onset. Time course of spreading depression is coincident with the negative shift in the DC potential (*lower*); tissue resistance in this slice (*upper*) rose to a ceiling of ~130% control.

TABLE 3. *Effect of osmolality on interictal bursts*

Change in Osmolality, mosmol/kg†	Interictal Burst, % Control*		
	Frequency	CA3 intensity	CA1 intensity‡
Hyperosmotic media			
Pooled Impermeant, +15, 30	98 ± 1.5 (79)	83 ± 1.9 (62)§	67 ± 5.1 (11)§
Pooled Permeant, +30	98 ± 1.2 (40)	101 ± 2.0 (38)	103 ± 7.4 (9)
Hypoosmotic media, −15	96 ± 2.6 (11)	134 ± 5.2 (11)§	159 ± 13.3 (10)§

Numbers in parentheses represent number of slices. *Burst intensity was estimated from coastline burst index. All burst parameters are percent of average of control and recovery values ± SE. There was no significant difference between values from slices in which hyperosmotic media did and did not abolish seizures, or between slices that were and were not undergoing electrographic seizure (power for 15% change was >0.67). Data were drawn from experiments with impermeant compounds mannitol (n = 42 slices), sucrose (n = 13), raffinose (n = 9), L-glucose (n = 7), dextran (n = 8); or permeant D-glucose (n = 15) and glycerol (n = 25). †Hyperosmotic changes were imposed by direct addition of appropriate amount of compound to the media. Media were made 15 mosmol hypoosmotic by removal of 7.5 mM NaCl (see METHODS) and recovery recorded following replacement of NaCl (n = 9) or addition of 15 mM mannitol (n = 2). Hypoosmotic media reversibly produced seizures in one slice. ‡CA1 burst intensity was evaluated only in slices not undergoing electrographic seizure, because bursts intensified prior to seizure initiation (66). §$P < 0.05$; significantly different from 100%; Student's t test.

changes in neuronal firing patterns and similar in magnitude to hyperosmotic changes observed for differential voltage deflections.

Tissue resistance and electrographic seizures

To determine whether the volume of extracellular space decreased during K^+-induced seizures, tissue resistance was measured in 12 slices undergoing a total of 286 electrographic seizures. Consistent with previous results from in situ experimental models (11), tissue resistance rose during the initial 15 s of seizure to 108 ± 0.4% of the value 20 s before seizure onset ($P < 0.001$; Fig. 4*A1*). For comparison, tissue resistance was also measured over episodes of spreading depression, during which brain tissue swells (48). Similar to findings in cortex (70), tissue resistance increased to a ceiling of 122 ± 4.4% (n = 5 slices; $P < 0.01$; Fig. 4*B*) during spreading depression induced by either brief (<1 s), orthodromic, electrical stimulation (200 Hz, 100 μA) or by hypoosmotic insult to the subiculum.

Examination of tissue resistance over the interseizure interval revealed a statistically significant trend toward an increase in resistance leading up to seizure initiation. This gradual increase was apparent when resistance measurements were made over many seizures, expressed relative to the value 20 s prior to seizure, and averaged together within each slice to minimize variability (see METHODS). In 6 of 12 slices, linear regression of the averaged values over the 20 s immediately preceding seizure revealed that tissue resistance was significantly correlated with time ($P < 0.001$) and gradually rose; no slices demonstrated a significant drop in resistance over the same period. When these averaged records from 12 individual slices were combined to form a composite time course of tissue resistance (see METHODS), the small increase in tissue resistance became more evident (Fig. 4*A2*). Linear regression of these values during the 20 s prior to seizure initiation in the final average (r = 0.871; $P < 0.001$) revealed a steady increase in tissue resistance with a slope of 0.07%/s. That is, approximately one-quarter of the resistance increase observed during seizures occurred before seizure initiation. The increased variability near seizure initiation resulted from a rapid increase of tissue resistance in several slices, rather than a decrease in the stability of the measure. Although tissue resistance increased only 1.6% prior to seizures, it might still reflect a critical change in extracellular space that could contribute to seizure initiation. Indeed, the lowest concentration of mannitol (5 mM) sufficient to abolish seizures reduced tissue resistance by only 1.2% (Table 2).

Hyperosmotic effects on interictal bursts and synaptic transmission

One possible way hyperosmolality might terminate seizures is through attenuation of interictal bursts, because in 1.5 mM $[Ca^{2+}]_o$ and $[Mg^{2+}]_o$, CA1 electrographic seizures were dependent on synaptic interictal input (65). Reductions in burst intensity could occur if hyperosmotic expansion of the extracellular space reduced synaptic transfer in the CA3 initiator region or at excitatory CA3-CA1 connections; osmolality is known to influence synaptic transmission in the periphery (34, 39, 71). Additionally, computer modeling of interictal bursts in $GABA_A$ antagonists predicts that ephaptic interactions substantially contribute to the amplitude of population spikes within a burst (64). We thus examined the effect of hyperosmolality on interictal bursts.

Alterations in osmolality did not influence interictal burst frequency, irrespective of the presence of electrographic seizures (Table 3). However, hyperosmolality induced by agents restricted to the extracellular space moder-

TABLE 4. *Effects of hyperosmolality on excitatory synaptic transmission in CA1*

Increase in Osmolality, mosmol/kg	Slope of Fiber Volley – Field EPSP Curve, % Control*	
	3.5 mM $[K^+]_o$	8.5 mM $[K^+]_o$
Mannitol, +15	90.3 ± 5.2 (10)	85.5 ± 6.1 (10)†
Glycerol, +30	102 ± 5.2 (7)	101 ± 5.4 (7)

Values are expressed as means ± SE. Numbers in parentheses represent number of slices. *Field EPSP was plotted as a function of presynaptic fiber volley amplitude (volley-EPSP curve; see METHODS), and slope of a line fit to initial portion of this relationship was calculated for control, experimental, and recovery periods. †$P < 0.05$; significantly different from 100%; Student's t test. Power to detect a real 10% change was >0.65.

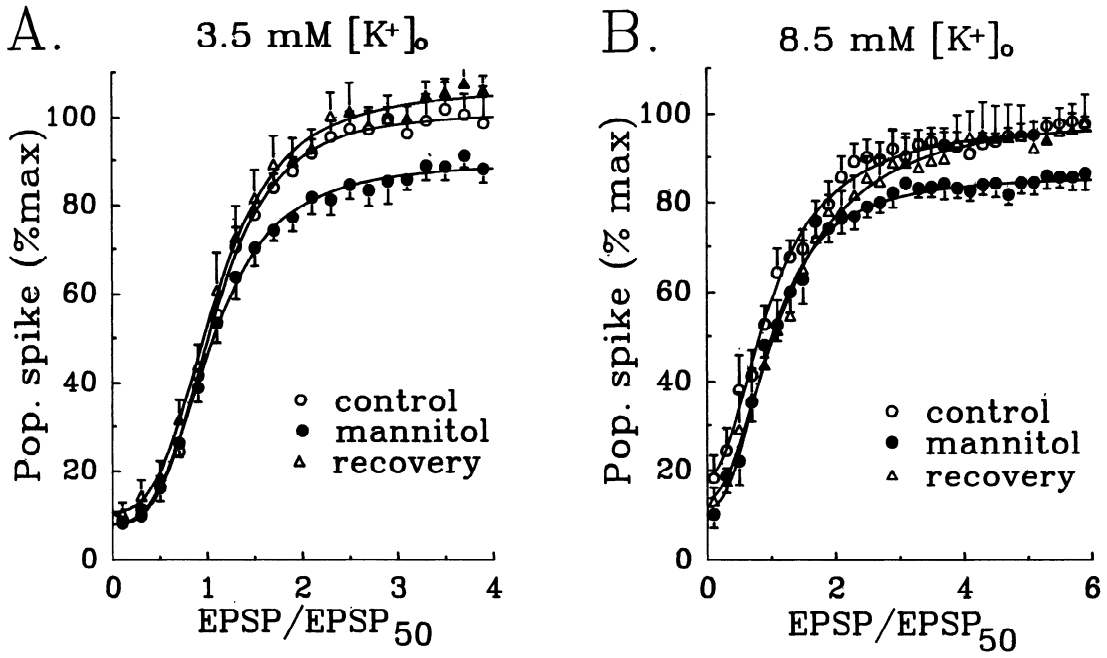

FIG. 5. Effect of hyperosmolality on EPSP-spike coupling. *A*: plots of composite EPSP-Spike curves were constructed (see METHODS) from data describing the effects of mannitol on EPSP-spike coupling in slices bathed in 3.5 (*A*; $n = 10$ slices) and 8.5 mM $[K^+]_o$ (*B*; $n = 8$ slices). Population spikes were normalized to their maximal value; EPSPs were expressed as a ratio to that which elicited a half-maximal population spike ($EPSP_{50}$). Error bars indicate SE; curves were fit as described in METHODS.

ately diminished CA3 and CA1 interictal burst intensity in both slices that were and were not undergoing electrographic seizures (Table 3). Conversely, media made hypoosmotic by removal of 7.5 mM NaCl increased burst intensity as expected if such treatment produced tissue swelling (Table 3). Analysis of CA3 burst waveforms indicated that neither hypo- nor hyperosmolality ($n = 7$ and 9 slices, respectively) markedly influenced burst duration, because the average number of population spikes within individual bursts never changed by more than one, the limit of resolution from background noise.

We examined input-output curves constructed from field potential recordings to determine if the observed hyperosmotic decrease in CA1 burst intensity might result from attenuation of excitatory transmission at the Schaffer-CA1 synapse or reduction in CA1 EPSP-spike coupling. Elevation of $[K^+]_o$ from 3.5 to 8.5 mM steepened the slope of the presynaptic volley-EPSP curve to 193 ± 30% of that in 3.5 mM $[K^+]_o$ ($n = 7$; $P < 0.05$) and shifted the EPSP-spike curve 3.4-fold to the left, as previously described (30). The slope of the volley-EPSP curve was only slightly reduced by mannitol, more so in 8.5 than 3.5 mM $[K^+]_o$ (Table 4). Likewise, hyperosmotic manipulations with mannitol (15 mosmol/kg) did not influence the lateral position of the EPSP-spike curve (Fig. 5). However, this concentration of mannitol significantly reduced the maximum population spike amplitude by 12–15% in both 3.5 and 8.5 mM $[K^+]_o$ (Fig. 5) Glycerol (30 mosmol/kg) had little influence on the volley-EPSP relationship (Table 4) or the position of EPSP-spike curves in either 3.5 or 8.5 mM $[K^+]_o$ ($n = 6$ and 5 slices, respectively; data not shown).

One additional means by which hyperosmotic expansion of the extracellular space might reduce excitability would be to decrease fiber diameter and, consequently, decrease axonal excitability and conduction velocity (e.g., Ref. 59). Small observed decreases in the slope of the relationship between stimulus intensity and fiber volley amplitude, however, were not statistically significant ($n = 6$ slices).

DISCUSSION

The most important conclusion of this study is that reduction of extracellular space is a critical component of the sequence of events that leads to electrographic seizure initiation in hippocampal slices bathed in high $[K^+]_o$. This conclusion rests on two independent lines of evidence. First, small increases (2.0–10.3%) in osmolality produced by compounds that are essentially impermeable to the plasma membrane rapidly and reliably abolished electrographic seizures and also reduced the electrical resistance of CA1 stratum pyramidale. Second, tissue resistance in CA1 increased markedly during seizures, but also gradually prior to seizure initiation (Fig. 4). We interpret the observed increase in tissue resistance to reflect a reduction in the extracellular volume (see below). Consequently, these results suggest that hyperosmolality prevents seizure initiation in this model by simply expanding extracellular space. The variety of chemical structures that were effective further implies that seizure suppression is unlikely to be due to effects other than osmolality, whereas the equivalence of three concentrations of mannitol and sucrose underscores the sensitivity of seizure threshold to even slight changes in extracellular space (Table 1).

Increases in tissue resistance during seizures reached about one-third of that observed during spreading depression and suggest that cells swell during seizure activity,

consistent with observations made in situ (e.g., Ref. 25). The resultant decreases in extracellular space during electrographic seizures probably produce excitatory effects that contribute to the maintenance of seizure activity. However, our observation of a small rise in tissue resistance over the 20 s immediately prior to seizure initiation indicates that a reduced extracellular volume could also contribute to events that lead up to seizure initiation. The similarity between the magnitude of resistance increase prior to seizure initiation (+1.6%) and the decrease in tissue resistance associated with hyperosmotic seizure suppression by 5 mM mannitol (−1.2%) further supports this conclusion.

Interpretation of resistance measurements

Tissue resistance, as measured here, reflects the resistance to current flow in extra- and intracellular paths (18), which will be considered in turn. Because most of the collisions that ions undergo within the narrow 20-nm clefts between cells in the CNS are with solvent molecules, the behavior of ions in interstitial fluid is approximately that in free solution (see Ref. 43). Accordingly, the contribution of extracellular resistance to the electrical resistance of tissue to current flow is a function of extracellular volume and tortuosity, as well as ionic strength and constituent ion mobilities (42). The proportion of an imposed current that traverses intracellular paths depends on membrane conductance, intracellular volume, and the mobility of ions within the cytoplasm. Trans- and intracellular resistance should be greater than interstitial resistance because of the higher resistance to current flow across plasma membranes versus within CSF, and also the reduction of ion mobilities that results from the two- to threefold higher viscosity of cytoplasm in comparison with CSF (35, 38). Therefore, the majority of an imposed current within tissue likely flows through extracellular paths. Consequently, changes in measured tissue resistance have long been interpreted as representative primarily of the extracellular resistance and, therefore, extracellular volume. However, this interpretation requires some caution, because changes in membrane conductance or the ionic composition of the CSF during neuronal activity can change the relative current flow through various paths. For example, K^+ moves primarily through glia rather than within the extracellular space (19), and any increases in $[K^+]_o$ will increase transglial currents. The resulting decrease in the ratio of extra- to intracellular current flow will cause the measurements of overall tissue resistance to underestimate changes in extracellular resistance.

The temporal resolution of the method used here is better than that achieved with measurement of extracellular diffusion profiles using ion-selective electrodes (42) and is well-suited for time periods <1 min. Small (e.g., 1–5%) changes could be detected by averaging a large number of observations, an approach that yielded quite reproducible results. We have interpreted the observed hyperosmotic reduction in tissue resistance in slices not undergoing electrographic seizures as reflecting an increase in extracellular space, because neuronal activity and probably base-line $[K^+]_o$ are relatively stable under these conditions. Whereas the elevated $[K^+]_o$ during seizures and during the 20 s prior to seizure onset should increase the ratio of intra- to extracellular current flow, such an effect cannot account for the increased tissue resistance, because it would produce an apparent decrease in resistance. Thus increases in tissue resistance in slices undergoing seizures seem likely to reflect a decrease in extracellular volume, which might be expected if the observed rise in $[K^+]_o$ (8, 66) induced glial swelling during this time. However, cautious interpretation is warranted for the measurements made over the interseizure interval because of the small magnitude of the increase.

Extracellular space and neuronal synchrony

How might reduction of extracellular space increase neuronal excitability and promote seizure initiation in this model? Reductions in extracellular space should exaggerate transient elevations in $[K^+]_o$ that can occur during periods of intense neuronal activity and also should enhance at least three different mechanisms by which electric fields can synchronize neuronal discharge. First, the momentary negative extracellular potential that occurs during an action potential will reduce the transmembrane potential of neurons within the voltage field, an effect that should be enhanced if excitable membranes move closer to the activated field source. Second, the voltage gradient that exists when cortical neurons fire synchronously will create an electric current, part of which will traverse the membranes of neighboring cells (16, 32, 62). The proportion of transmembrane current will increase as the extracellular resistance rises in swollen tissue (12) and as excitable membranes move closer to the field source (each other). Calculation of the distance over which electrical interactions occur is complicated. However, the observation of 5- to 20-mV field potentials recorded from micropipettes with ~5 μm tip diameter, or of unit spikes with sharper electrodes, indicates that the effective range of such fields must be many microns, well in excess of the distance separating neurons. Indeed, Jefferys (27) has shown that the magnitude of field potentials in the hippocampus is sufficient to increase neuronal recruitment during orthodromic stimulation. A third consequence of voltage gradients extending over the extracellular space would be a transient redistribution of the concentrations of the major charge carriers (Na^+ and Cl^-) near activated neurons, which might influence the excitability of adjacent neurons in various ways. Although the relative contribution of these mechanisms to tissue synchrony is unknown, overall electric field effects have important consequences in regions like CA1 stratum pyramidale, in which some excitable membranes are separated by only interstitial space rather than intervening processes or glia.

Such ephaptic excitation can powerfully enhance neuronal synchrony and, under some circumstances, appears sufficient to synchronize neuronal firing. For example, synchronous epileptiform discharges appear in hippocampal slices in which synaptic transmission is blocked by removal of $[Ca^{2+}]_o$ (21, 31, 62). Electric field depolarizations can be directly observed in CA1 neurons during this synchronous activity by comparison of the transmembrane potential to the field potential, and appear as subthreshold depolariza-

tions coincident with population spikes (21, 62). Similar ephaptic depolarizations associated with antidromic population spikes can surpass EPSP amplitude (13).

Interictal bursts and synaptic transmission

It is difficult to determine how much of the observed 15–30% decreases in interictal burst intensity produced by hyperosmotic media reflect real changes in neuronal firing or, rather, are consequences of reductions in tissue resistance. In the CA3 region, burst intensity was attenuated by ~15%, whereas tissue resistance decreased 5–10%. Accordingly, a substantial portion of the estimated decrease in burst intensity probably reflects reductions in population spike amplitude according to Ohm's Law. This interpretation is consistent with the insensitivity of burst frequency and waveform in the CA3 burst generator to hyperosmotic manipulations, even in slices in which seizures were abolished (Table 3). In contrast, the ~30% reduction in CA1 burst intensity (Table 3) in response to hyperosmotic changes that decreased tissue resistance 5–10% cannot simply be a consequence of Ohm's Law, but rather indicates a real reduction in neuronal firing. Likewise, the reversible 10–15% decrease in maximum CA1 population spike amplitude (Fig. 5) produced by 15 mM mannitol is probably caused by factors in addition to the ~5% decrease in tissue resistance produced by this concentration of mannitol. Ephaptic excitation has been previously suggested to contribute significantly to neuronal recruitment within a burst (64) and also to increase the amplitude of a single orthodromic population spike (13). Hence, a reduction in electric field effects in hyperosmotic media might account for a substantial portion of the observed reduction in CA1 burst intensity and EPSP-spike coupling, and this could contribute to the prevention of CA1 seizures.

The slight reduction in field EPSP amplitude in response to a given fiber volley in hyperosmotic media (Table 4) suggests that excitatory synaptic transmission might be impaired, which could contribute to reduction of burst intensity and seizure suppression. However, the observation that seizures in slices bathed in 1.2 mM $[Ca^{2+}]_o$ and $[Mg^{2+}]_o$ were independent of a synaptic trigger (65), yet were still sensitive to hyperosmolality, suggests that expansion of the extracellular space exerts important actions on mechanisms apart from synaptic transmission. Moreover, preliminary reports that indicate both membrane potential and input resistance are insensitive to osmolality (2) further imply that hyperosmolality attenuates neuronal excitability by reducing electric field interactions.

Control of seizure initiation

A number of events within the CA1 region are correlated with the increasing burst intensity prior to seizure onset, and seizure initiation itself. These include NMDA receptor activation, neuronal depolarization, and an increase in $[K^+]_o$ (8, 66). We have previously combined these data with other known consequences of elevated $[K^+]_o$ to produce an hypothesis for the transition from interictal to ictal events within CA1 (66). A logical prediction given the initially high (8.5 mM) $[K^+]_o$ is that glial swelling and decreased extracellular space would augment tissue excitability and that enhanced ephaptic interactions provide a crucial synchronizing trigger for seizure initiation. Our observations of hyperosmotic seizure suppression and increasing tissue resistance prior to seizure initiation together suggest that a subtle reduction in extracellular space is, indeed, a critical determinant of the conditions that enable CA3 interictal input to precipitate an electrographic seizure in CA1. Increasing electric field interactions over the interseizure interval, and to a lesser extent increasing synaptic excitation, probably recruits more neurons into each subsequent interictal burst. Such a process could become regenerative and lead to the explosive increase in interictal burst intensity that usually reaches 400% of control as CA1 progresses to seizure (66). Thus the threshold level of $[K^+]_o$ necessary to induce significant glial swelling in hippocampal slices is a critical issue. Although cerebral cortex in cat appears to swell when $[K^+]_o$ reaches a threshold of ~10 mM (4), it is not clear how hippocampal cells respond to graded changes in $[K^+]_o$. Perhaps a reduced $[K^+]_o$ threshold for glial swelling in hippocampus contributes to the long-suspected seizure susceptibility of this structure.

It has been difficult to assess the relative contribution of events associated with seizure initiation and maintenance. Yet, the speed and reliability with which small increases in osmolality suppress seizures is consistent with reductions in extracellular volume being a key contributing factor to seizure initiation. For example, hyperosmolality blocked seizures in a somewhat higher fraction of slices than did the competitive NMDA antagonist D-APV (66). Furthermore, hyperosmolality abolished electrographic seizures in three slices that were resistant to D-APV (Table 1). Thus both electric field effects and synaptic excitation appear to critically contribute to seizure initiation in CA1 neurons in slices.

These and other experimental results (11, 73) raise the possibility that manipulation of extracellular space could be a promising therapeutic approach to the treatment of status epilepticus, hypoxic seizures, or perhaps some forms of epilepsy. This idea is supported by data that suggest synchronous discharges occurring in the absence of $[Mg^{2+}]_o$ are sensitive to hyperosmolality (2). In addition, brain edema appears present during kainate-induced seizures (41), and Baran et al. (3) have noted that intravenous mannitol could suppress kainate seizures in rats, despite the potential transfer of K^+ from plasma to neural tissue that can occur with blood-brain barrier disruption (7).

We thank N. Chamberlin and Dr. F. E. Dudek for helpful comments.

This work was supported by National Institute of Neurological and Communicative Disorders and Stroke Grant NS-17771 and a National Science Foundation Predoctoral Fellowship to S. Traynelis, and was completed in partial fulfillment of the requirements for the degree of Doctor of Philosophy in Pharmacology.

Address reprint requests to S. F. Traynelis.

Received 9 September 1988; accepted in final form 20 December 1988.

REFERENCES

1. ALGER, B. E. AND NICOLL, R. A. Epileptiform burst afterhyperpolarization: calcium-dependent potassium potential in hippocampal CA1 pyramidal cells. *Science Wash. DC* 210: 1122–1124, 1980.
2. BALLYK, B. A. AND ANDREW, R. D. Inverse relation between CA1

excitability and osmolality in hippocampal slice. *Soc. Neurosci. Abstr.* 14: 572, 1988.
3. BARAN, H., LASSMANN, H., SPERK, G., SEITELBERGER, F., AND HORNYKIEWICZ, O. Effect of mannitol treatment on brain neurotransmitter markers in kainic acid-induced epilepsy. *Neuroscience* 21: 679–684, 1987.
4. BOURKE, R. S. AND NELSON, K. M. Further studies on the K^+-dependent swelling of primate cerebral cortex *in vivo:* the enzymatic basis of the K^+-dependent transport of chloride. *J. Neurochem.* 19: 663–685, 1972.
5. CARLSEN, A. AND WIETH, J. O. Glycerol transport in human red cells. *Acta Physiol. Scand.* 97: 501–513, 1976.
6. CLAUSEN, T., DAHL-HANSEN, A. B., AND ELBRINK, J. The effect of hyperosmolarity and insulin on resting tension and calcium fluxes in rat soleus muscle. *J. Physiol. Lond.* 292: 505–526, 1979.
7. CSERR, H. F., DEPASQUALE, M., AND PATLAK, C. S. Volume regulatory influx of electrolytes from plasma to brain during acute hyperosmolality. *Am. J. Physiol.* 253 (*Renal Fluid Electrolyte Physiol.* 21): F530–F537, 1987.
8. DAVID, G., YAARI, Y., AND JENSEN, M. S. Potassium-induced tonic-clonic seizures in the mammalian in vitro hippocampus. *Soc. Neurosci. Abstr.* 13: 1154, 1987.
9. DICHTER, M. A., HERMAN, C. J., AND SELZER, M. Silent cells during interictal discharges and seizures in hippocampal penicillin foci. Evidence for the role of extracellular K^+ in the transition from the interictal state to seizures. *Brain Res.* 48: 173–183, 1972.
10. DICK, A. P. K. AND HARIK, S. I. Distribution of the glucose transporter in the mammalian brain. *J. Neurochem.* 46: 1406–1411, 1986.
11. DIETZEL, I., HEINEMANN, U., HOFMEIER, G., AND LUX, H. D. Transient changes in the size of the extracellular space in the sensorimotor cortex of cats in relation to stimulus-induced changes in potassium concentration. *Exp. Brain Res.* 40: 432–439, 1980.
12. DUDEK, F. E., SNOW, R. W., AND TAYLOR, C. P. Role of electrical interactions in synchronization of epileptiform bursts. *Adv. Neurol.* 44: 593–617, 1986.
13. DUDEK, F. E., GRIBKOFF, V. K., AND CHRISTIAN, E. P. Mechanisms of potentiation independent of chemical synapses. In: *Long-Term Potentiation: From Biophysics to Behavior,* edited by P. W. Landfield and S. A. Deadwyler. New York: Liss, 1988, p. 439–464.
14. FERTZIGER, A. P. AND RANCK, J. B., JR. Potassium accumulation in interstitial space during epileptiform seizures. *Exp. Neurol.* 26: 571–585, 1970.
15. FISHER, R. S., PEDLEY, T. A., MOODY, W. J., AND PRINCE, D. A. The role of extracellular potassium in hippocampal epilepsy. *Arch. Neurol.* 33: 76–83, 1976.
16. FURUKAWA, T. AND FURSHPAN, E. J. Two inhibitory mechanisms in the mauthner neurons of goldfish. *J. Neurophysiol.* 26: 140–176, 1963.
17. GALVAN, M., GRAFE, P., AND TEN BRUGGENCATE, G. Convulsant actions of 4-amino-pyridine on the guinea-pig olfactory cortex slice. *Brain Res.* 241: 75–86, 1984.
18. GARDNER-MEDWIN, A. R. Membrane transport and solute migration affecting the brain cell microenvironment. *Neurosci. Res. Program Bull.* 18: 208–226, 1980.
19. GARDNER-MEDWIN, A. R. A study of the mechanisms by which potassium moves through brain tissue in the rat. *J. Physiol. Lond.* 335: 353–374, 1983.
20. GJEDDE, A. High- and low-affinity transport of D-glucose from blood to brain. *J. Neurochem.* 36: 1463–1471, 1981.
21. HAAS, H. L. AND JEFFERYS, J. G. R. Low-calcium field burst discharges of CA1 pyramidal neurones in rat hippocampal slices. *J. Physiol. Lond.* 354: 185–201, 1984.
22. HABLITZ, J. J. Spontaneous ictal-like discharges and sustained potential shifts in the developing rat neocortex. *J. Neurophysiol.* 58: 1052–1065, 1987.
23. HARA, M., MATSUDA, Y., AND NAKAGAWA, H. Molecular characteristics of rat brain glucose transporter: a novel species with M_r 45,000. *J. Biochem. Tokyo* 101: 43–52, 1987.
24. HEINEMANN, U., KONNERTH, A., PUMAIN, R., AND WADMAN, W. J. Extracellular calcium and potassium concentration changes in chronic epileptic brain tissue. *Adv. Neurol.* 44: 641–661, 1986.
25. HEINEMANN, U. AND DIETZEL, I. Extracellular potassium concentrations in chronic alumina cream foci of cats. *J. Neurophysiol.* 52: 421–434, 1984.
26. HOLSHEIMER, J. Electrical conductivity of the hippocampal CA1 layers and application to current-source-density analysis. *Exp. Brain Res.* 67: 402–410 1987.
27. JEFFERYS, J. G. R. Influence of electric fields on the excitability of granule cells in guinea-pig hippocampal slices. *J. Physiol. Lond.* 319: 143–152, 1981.
28. JEFFERYS, J. G. R. AND HAAS, H. L. Synchronized bursting of CA1 hippocampal pyramidal cells in the absence of synaptic transmission. *Nature Lond.* 300: 448–450, 1982.
29. KIMELBERG, H. K. AND FRANGAKIS, M. V. Furosemide- and bumetanide-sensitive ion transport and volume control in primary astrocyte cultures from rat brain. *Brain Res.* 361: 125–134, 1985.
30. KING, G. L., DINGLEDINE, R., GIACCHINO, J. L., AND MCNAMARA, J. O. Abnormal neuronal excitability in hippocampal slices from kindled rats. *J. Neurophysiol.* 54: 1295–1304, 1985.
31. KONNERTH, A., HEINEMANN, U., AND YAARI, Y. Slow transmission of neural activity in hippocampal area CA1 in absence of active chemical synapses. *Nature Lond.* 307: 69–71, 1984.
32. KORN, H. AND FABER, D. S. An electrically mediated inhibition in goldfish medulla. *J. Neurophysiol.* 38: 452–471, 1975.
33. KORN, S. J., GIACCHINO, J. L., CHAMBERLIN, N. L., AND DINGLEDINE, R. Epileptiform burst activity induced by potassium in the hippocampus and its regulation by GABA-mediated inhibition. *J. Neurophysiol.* 57: 325–340, 1987.
34. KRIEBEL, M. E. AND PAPPAS, G. D. Effect of hypertonic saline on quantal size and synaptic vesicles in identified neuromuscular junction of the frog. *Neuroscience* 23: 745–756, 1987.
35. KUSHMERICK, M. J. AND PODOLSKY, R. J. Ionic mobility in muscle cells. *Science Wash. DC* 166: 1297–1298, 1969.
36. LI, C.-C. AND LIN, E. C. C. Glycerol transport and phosphorylation by rat hepatocytes. *J. Cell. Physiol.* 117: 230–234, 1983.
37. MACVICAR, B. A., BAKER, K., AND CRICHTON, S. A. Kainic acid evokes a potassium efflux from astrocytes. *Neuroscience* 25: 721–725, 1988.
38. MASTRO, A. M. AND KEITH, A. D. Diffusion in the aqueous compartment. *J. Cell. Biol.* 99: 180s–187s, 1984.
39. MCGRATH, M. A. AND SHEPHERD, J. T. Hyperosmolarity: effects on nerves and smooth muscle of cutaneous veins. *Am. J. Physiol.* 231: 141–147, 1976.
40. MISGELD, U. DEISZ, R. A., DODT, H. U., AND LUX, H. D. The role of chloride transport in postsynaptic inhibition of hippocampal neurons. *Science Wash. DC* 232: 1413–1415, 1986.
41. NELSON, S. R. AND OLSON, J. P. Role of early edema in the development of regional seizure-related brain damage. *Neurochem. Res.* 12: 561–564, 1987.
42. NICHOLSON, C. AND PHILLIPS, J. M. Ion diffusion modified by tortuosity and volume fraction in the extracellular microenvironment of cat cerebellum. *J. Physiol. Lond.* 321: 225–257, 1981.
43. NICHOLSON, C. AND RICE, M. E. The migration of substances in the neuronal microenvironment. *Ann. NY Acad. Sci.* 481: 55–71, 1986.
44. NOWAK, L., BREGESTOVSKI, P., ASCHER, P., HERBERT, A., AND PROCHIANTZ, A. Magnesium gates glutamate-activated channels in mouse central neurones. *Nature Lond.* 307: 462–465, 1984.
45. OHNO, K., PETTIGREW, K. D., AND RAPOPORT, S. I. Lower limits of cerebrovascular permeability to nonelectrolytes in the conscious rat. *Am. J. Physiol.* 235 (*Heart Circ. Physiol.* 3): H299–H307, 1978.
46. PAPPIUS, H. M. AND ELLIOTT, K. A. C. Water distribution in incubated slices of brain and other tissues. *Can. J. Biochem. Physiol.* 34: 1007–1022, 1956.
47. PETRONINI, P. G., TRAMACERE, M., KAY, J. E., AND BORGHETTI, A. F. Adaptive response of cultured fibroblasts to hyperosmolarity. *Exp. Cell Res.* 165: 180–190, 1986.
48. PHILLIPS, J. M. AND NICHOLSON, C. Anion permeability in spreading depression investigated with ion sensitive-microelectrodes. *Brain Res.* 173: 567–571 1979.
49. POLLAY, M., FULLENWIDER, C., ROBERTS, P. A., AND STEVENS, F. A. Effect of mannitol and furosemide on blood-brain osmotic gradient and intracranial pressure. *J. Neurosurg.* 59: 945–950, 1983.
50. POOLOS, N. P. MAUCK, M. D., AND KOCSIS, J. D. Activity-evoked increases in extracellular potassium modulate presynaptic excitability in the CA1 region of the hippocampus. *J. Neurophysiol.* 58: 404–416, 1987.
51. RANSOM, B. R., YAMATE, C. L., AND CONNORS, B. W. Activity-dependent shrinkage of extracellular space in rat optic nerve: a developmental study. *J. Neurosci.* 5: 532–535, 1985.

52. RUTECKI, P. A., LEBEDA, F. J., AND JOHNSTON, D. Epileptiform activity induced by changes in extracellular potassium in hippocampus. *J. Neurophysiol.* 54: 1363–1374, 1985.
53. SISSON, W. B. AND OLDENDORF, W. H. Brain distribution spaces of mannitol-^{3}H, inulin-^{14}C, and dextran-^{14}C in the rat. *Am. J. Physiol.* 221: 214–217, 1971.
54. SKOU, J. C. Further investigations on a Mg^{++} + Na^{+}-activated adenosine-triphosphatase, possibly related to active, linked transport of Na^{+} and K^{+} across nerve membranes. *Biochim. Biophys. Acta* 42: 6–23, 1960.
55. SOMJEN, G. G. Interstitial ion concentration and the role of neuroglia in seizures. In: *Electrophysiology of Epilepsy,* edited by P. A. Schwartzkroin and H. V. Wheal. London: Academic, 1984, p. 304–341.
56. SOMJEN, G. G., AITKEN, P. G., AND GIACCHINO, J. L. Sustained potential shifts and paroxysmal discharges in hippocampal formation. *J. Neurophysiol.* 53: 1079–1097, 1985.
57. SOMJEN, G. G. AND GIACCHINO, J. L. Potassium and calcium concentrations in interstitial fluid of hippocampal formation during paroxysmal responses. *J. Neurophysiol.* 53: 1098–1108, 1985.
58. STERRETT, P. R., THOMPSON, A. M., CHAPMAN, A. L., AND MATZKE, H. A. The effects of hyperosmolarity on the blood-brain barrier. A morphological and physiological correlation. *Brain Res.* 77: 281–295, 1974.
59. SUGIMARA, K., WINDEBANK, A. J., NATARAJAN, V., LAMBERT, E. H., SCHMID, H. H. O., AND DYCK, P. J. Interstitial hyperosmolarity may cause axis cylinder shrinkage in streptozotocin diabetic nerve. *J. Neuropathol. & Exp. Neurol.* 39: 710–21, 1980.
60. SWANN, J. W. AND BRADY, R. J. Penicillin-induced epileptogenesis in immature rat CA3 hippocampal pyramidal cells. *Dev. Brain Res.* 12: 243–254, 1984.
61. SZERB, J. C. AND O'REGAN, P. A. Reversible shifts in the Ca^{2+}-dependent release of aspartate and glutamate from hippocampal slices with changing glucose concentrations. *Synapse* 1: 265–272, 1987.
62. TAYLOR, C. P. AND DUDEK, F. E. Synchronous neural afterdischarges in rat hippocampal slices without active chemical synapses. *Science Wash. DC* 218: 810–812, 1982.
63. THURSTON, J. H., HAUHART, R. E., AND DIRGO, J. A. Effects of a single therapeutic dose of glycerol on cerebral metabolism in the brains of young mice: possible increase in brain glucose transport and glucose utilization. *J. Neurochem.* 36: 830–838, 1981.
64. TRAUB, R. D., DUDEK, F. E., SNOW, R. W., AND KNOWLES, W. D. Computer simulations indicate electrical field effects contribute to the shape of the epileptiform field potential. *Neuroscience* 15: 947–958, 1985.
65. TRAYNELIS, S. F. AND DINGLEDINE, R. Modification of potassium-induced interictal bursts and electrographic seizures by divalent cations. *Neurosci. Lett.* In press.
66. TRAYNELIS, S. F. AND DINGLEDINE, R. Potassium-induced spontaneous electrographic seizures in the rat hippocampal slice. *J. Neurophysiol.* 59: 259–276, 1988.
67. TRAYNELIS, S. F. AND DINGLEDINE, R. Spontaneous electrographic seizures in hippocampal slices bathed in high external potassium are suppressed by hyperosmotic media. *Neurosci. Lett. Suppl.* 32: S36, 1988.
68. TRAYNELIS, S. F. AND DINGLEDINE, R. Spontaneous high $[K^{+}]_o$-induced electrographic seizures in hippocampal slices are suppressed by hyperosmotic media. *Soc. Neurosci. Abstr.* 14: 471, 1988.
69. VALENTINO, R. J. AND DINGLEDINE, R. Pharmacological characterization of opioid effects in the rat hippocampal slice. *J. Pharmacol. Exp. Ther.* 223: 502–509, 1982.
70. VAN HARREVELD, A. AND OCHS, S. Electrical and vascular concomitants of spreading depression. *Am. J. Physiol.* 189: 159–166, 1957.
71. VAN DER KLOOT, W. Pretreatment with hypertonic solutions increases quantal size at the frog neuromuscular junction. *J. Neurophysiol.* 57: 1536–1554, 1987.
72. WALZ, W. AND MUKERJI, S. KCl movements during potassium-induced cytotoxic swelling of cultured astrocytes. *Exp. Neurol.* 99: 17–29, 1988.
73. YAARI, Y., KONNERTH, A., AND HEINEMANN, U. Nonsynaptic epileptogenesis in the mammalian hippocampus in vitro. II. Role of extracellular potassium. *J. Neurophysiol.* 56: 424–438, 1986.
74. ZUCKERMANN, E. C. AND GLASER, G. H. Hippocampal epileptic activity induced by localized ventricular perfusion with high-potassium cerebrospinal fluid. *Exp. Neurol.* 20: 87–110 1968.